JOURNAL OF VIROLOGY, Feb. 1997, p. 1598–1607 Vol. 71, No. 2
0022-538X/97/$04.00+0

Functions of the Tobacco Etch Virus RNA Polymerase (NIb): Subcellular Transport and Protein-Protein Interaction with VPg/Proteinase (NIa)

XIAO HUA LI, PATRICIA VALDEZ, REBECCA E. OLVERA, AND JAMES C. CARRINGTON*

Department of Biology, Texas A&M University, College Station, Texas 77843

Received 6 July 1996/Accepted 4 November 1996

The NIb protein of tobacco etch potyvirus (TEV) possesses several functions, including RNA-dependent RNA polymerase and nuclear translocation activities. Using a reporter protein fusion strategy, NIb was shown to contain two independent nuclear localization signals (NLS I and NLS II). NLS I was mapped to a sequence within amino acid residues 1 to 17, and NLS II was identified between residues 292 and 316. Clustered point mutations resulting in substitutions of basic residues within the NLSs were shown previously to disrupt nuclear translocation activity. These mutations also abolished TEV RNA amplification when introduced into the viral genome. The amplification defects caused by each NLS mutation were complemented in *trans* within transgenic cells expressing functional NIb, although the level of complementation detected for each mutant differed significantly. Combined with previous results (X. H. Li and J. C. Carrington, Proc. Natl. Acad. Sci. USA 92:457–461, 1995), these data suggest that the NLSs overlap with essential regions necessary for NIb *trans*-active function(s). The fact that NIb functions in *trans* implies that it must interact with one or more other components of the genome replication apparatus. A yeast two-hybrid system was used to investigate physical interactions between NIb and several other TEV replication proteins, including the multifunctional VPg/proteinase NIa and the RNA helicase CI. A specific interaction was detected between NIa and NIb. Deletion of any of five regions spanning the NIb sequence resulted in NIb variants that were unable to interact with NIa. Clustered point mutations affecting the conserved GDD motif or NLS II within the central region of NIb, but not mutations affecting NLS I near the N terminus, reduced or eliminated the interaction. The C-terminal proteinase (Pro) domain of NIa, but not the N-terminal VPg domain, interacted with NIb. The effects of NIb mutations within NLS I, NLS II, and the GDD motif on the interaction between the Pro domain and NIb were identical to the effects of these mutations on the interaction between full-length NIa and NIb. These data are compatible with a model in which NIb is directed to replication complexes through an interaction with the Pro domain of NIa.

The biochemical mechanisms involved in replication of genomes of positive-strand RNA viruses of eukaryotes are understood poorly. This statement is particularly applicable to members of the picornavirus supergroup. In large part, this is due to difficulties in reconstituting the complete picornavirus-like viral replicative cycle in vitro by using purified replication factors (53). A complete picture of how viral- and host-encoded factors and structures are coordinated during replication complex formation and RNA synthesis, therefore, has yet to emerge.

Tobacco etch potyvirus (TEV) is a well-characterized member of the *Potyviridae*. This family shares genome organizational features with other families within the picornavirus supergroup (32). The TEV genome is covalently attached to a virus-encoded protein, termed VPg, and encodes a large polyprotein of 346 kDa (1). At least nine mature proteins arise by proteolytic processing catalyzed by three TEV-encoded proteinases (16) (see Fig. 1A). Several proteins derived from the central region of the viral polyprotein, in the order CI-6K-NIa-NIb, are proposed to function directly in RNA replication. The CI protein contains nucleoside triphosphatase and RNA unwinding activities and exhibits sequence similarity with several known RNA helicases (34, 35). The 6-kDa protein is associated tightly with membranes and may serve to anchor RNA replication complexes to membranous sites of synthesis (46). The multifunctional NIa protein contains a VPg domain within the N-terminal half and a picornavirus 3C-like proteinase (Pro) domain proximal to the C terminus (8, 50). The NIb protein likely functions as the RNA-dependent RNA polymerase (1, 14). The CI-6K-NIa-NIb region of the polyprotein contains sequence and functional similarity with the 2C-3A-3B-3C-3D region of the picornavirus polyprotein (32, 53).

The NIa proteinase is required for proteolytic maturation of the majority of viral proteins (6–8, 20, 25). This enzyme exhibits *cis*-preferential proteolytic activity in vitro at several sites, including the CI/6K, 6K/NIa, and NIa/NIb cleavage sites, and *trans*-proteolytic activity at the P3-CI and NIb-capsid protein sites. Additionally, NIa catalyzes cleavage at an internal site between the VPg and Pro domains (15). Processing at the NIa internal site is extremely inefficient due to a suboptimal cleavage site motif flanking the scissile bond. Internal cleavage site-inactivating mutations, as well as mutations resulting in accelerated internal cleavage, are amplification debilitated (11, 49), suggesting that the slow processing characteristic of the internal site is an important regulatory feature. Both full-length NIa and the processed N-terminal domain have been detected as VPg molecules covalently bound to genomic RNA (11, 40).

Despite the requirement for NIa and NIb in the cytoplasm or membrane-bound replication complexes during proteolytic processing and viral RNA synthesis, the vast majority of NIa and NIb molecules are localized in the nucleus of infected cells

* Corresponding author. Phone: (409) 845-2325. Fax: (409) 845-2891. E-mail: carrington@bio.tamu.edu.

(5, 44). Both proteins contain independent nuclear localization signals (NLSs) (10, 37, 44). Localization of at least a subset of NIa and NIb molecules to membranous sites of replication was proposed to occur by at least two mechanisms. The NIa protein or VPg domain may be directed toward replication complexes through covalent association with the 6K protein in a polyprotein form. The membrane-binding activity of the 6K protein is sufficient to override the nuclear localization activity of NIa (45). By genetic complementation analysis, the NIb protein was shown to be a *trans*-active protein that can be supplied from outside the context of the TEV polyprotein (36). Therefore, NIb may be recruited to replication complexes through protein-protein interactions with other viral or host factors or by protein-RNA interactions (26, 36).

To investigate further the activities of NIb, nuclear transport requirements and interactions with other TEV-encoded protein were analyzed. Two independent NLSs were identified by using a reporter protein fusion approach. In addition, a combinatorial study of TEV protein-protein interactions by using the yeast two-hybrid system revealed that NIb interacted specifically with the Pro domain of NIa.

MATERIALS AND METHODS

Plasmid construction. Vectors containing regulatory sequences and coding regions for plant transformation were generated with pGA482 (2). pGA-GUS/NIb contains the sequence encoding a fusion protein consisting of β-glucuronidase (GUS) and NIb, while pGA-GUS contains the nonfused GUS coding sequence (37, 44). pGA-G/b.1-17 and pGA-G/b.292-316 contain the GUS sequence fused to the 5′ end of a cDNA fragment coding for either amino acids 1 to 17 or 292 to 316 of NIb, respectively.

As described previously, pTEV7DAN-GUS contains a full-length cDNA of the TEV genome with the GUS sequence inserted between the P1 and HC-Pro coding regions (12, 13). Clustered point mutations resulting in substitutions of Glu-Asp-Glu for Lys3-Arg4-Lys5 (EDE mutation), Asp-Asp for Lys303-Lys304 (DD mutation), and Val-Asn-Asn for Gly357-Asp348-Asp349 (VNN mutation) within the NIb sequence of pTEV7DAN-GUS were described elsewhere (36, 37).

Two shuttle plasmids, pAS2 and pACT2 (obtained from Stephen Elledge), containing the coding sequences for the GAL4 DNA-binding domain (DB) or transcriptional activation domain (ACT), respectively, were used for all yeast two-hybrid experiments (17, 18). Sequences coding for NIa, NIb, CI, or GUS were inserted into pAS2 at the 3′ end of the DB region, generating pAS.a, pAS.b, pAS.CI, or pAS.G, respectively. The same sequences were also inserted into pACT2 at the 3′ end of the ACT region, resulting in pACT.a, pACT.b, pACT.CI, or pACT.G, respectively. Sequences coding for the VPg domain (NIa codons 1 to 188) and Pro domain (NIa codons 189 to 430) were also subcloned into the two vectors, yielding pACT.VPg, pACT.Pro, pAS.VPg, and pAS.Pro.

The EDE, DD, and VNN mutations were introduced into the NIb coding sequence of pAS.b, resulting in pAS.EDE, pAS.DD, and pAS.VNN, respectively. Five deletions were prepared by oligonucleotide-directed loop-out mutagenesis (33). The sequences deleted were those for NIb codons 1 to 141 (bΔ1 mutation), 142 to 243 (bΔ2), 244 to 354 (bΔ3), 355 to 412 (bΔ4), and 413 to 512 (bΔ5). All deletions and modifications were confirmed by DNA sequence analysis.

Two plasmids, pSE1111 derived from pACT and pSE1112 derived from pAS1 (obtained from Stephen Elledge), encoded fusions with the yeast proteins SNF4 and SNF1, respectively. These proteins are known to interact in the yeast two-hybrid system (18) and were used as positive controls in several experiments. In all two-hybrid experiments, cells doubly transformed with the parental plasmids, pACT2 and pAS2, were analyzed in parallel with experimental samples.

Transgenic tobacco plants and subcellular localization of GUS activity. Transgenic plants expressing NIb (NIb^+), GUS, or GUS/NIb fusion protein were described previously (36, 37). *Nicotiana tabacum* cv. Xanthi nc and $Havana_{425}$ plants were transformed with pGA-G/b.1-17 and pGA-G/b.292-316 as described (9). Plant extracts were subjected to immunoblot analysis with anti-GUS serum (37). The distribution of GUS activity in leaf epidermal cells of original transformed plants and R_1 progeny plants was analyzed with the histochemical GUS substrate, X-Gluc (5-bromo-4-chloro-3-indolyl-β-D-glucuronic acid), as described (44).

In vitro synthesis of transcripts and inoculation of protoplasts and plants. Capped transcripts were synthesized with SP6 RNA polymerase (Ambion) as described (13). Protoplasts from leaves of either vector-transformed or NIb^+-expressing plants were inoculated with transcripts as detailed previously (36). GUS activity was analyzed in protoplasts 24, 48, and 72 h postinoculation (p.i.) (11). Transgenic NIb^+ or vector-transformed plants were also inoculated with transcripts. Systemically infected tissue was harvested as soon as symptoms developed (5 to 8 days p.i.) and ground in 5 volumes of 10 mM Tris-HCl–1 mM EDTA, pH 7.6. The extracts were used to inoculate vector- or NIb^+-transformed plants. Histochemical GUS activity assays were conducted with inoculated leaves at 3 days p.i.

Bacterial strains, yeast strains, and yeast transformation. *Escherichia coli* TG1 and DH5α and *Saccharomyces cerevisiae* Y190 [*MAT***a** *gal4 gal80 his3 trp1-901 ade2-101 ura3-52 leu2-3,-112/+ URA3*::*GAL*→*lacZ LYS2*::*GAL*(*UAS*)→*HIS3 cyh*^{r}] were used for all DNA cloning and expression. For yeast transformation, Y190 cells were grown at 30°C in YEPD liquid medium (1% yeast extract–2% peptone–2% glucose) to approximately 3×10^7 cells/ml, collected by centrifugation, washed with TE buffer (10 mM Tris-HCl [pH 7.6], 1 mM EDTA), and resuspended in TE at a density of 0.5×10^9 to 1.0×10^9 cells/ml. An equal volume of 0.2% LiCl was added to the cell suspension, and the mixture was incubated for 1 h at 30°C. Approximately 1 μg of plasmid DNA/150 μg of salmon testes carrier DNA (Sigma)/120 μl of 70% polyethylene glycol (molecular weight, 4,000; Fluka Chemika) was mixed with 100 μl of TE-LiCl cell suspension and incubated for 2 to 4 h at 30°C. After a 10-min heat shock at 42°C, 1 ml of TE was mixed with the transformation solution. Cells were sedimented by centrifugation for 1 min at $2{,}000 \times g$, resuspended in 100 μl of TE, and spread on 2% glucose-containing SC medium lacking leucine (SC-Leu) for pACT2-derived plasmids or lacking tryptophan (SC-Trp) for pAS2-derived plasmids. Cells from transformed colonies were then transformed with a second, counterpart plasmid by the same procedure as above, except that the cells were propagated in liquid SC-Leu or SC-Trp medium before transformation and plated on SC-Leu-Trp double selective medium after transformation. Transformed yeast cells were screened by immunoblot analysis using antisera against the respective TEV or control proteins or by PCR analysis with TEV- or plasmid-specific primers.

In some experiments, the pAS2-derived plasmid from doubly transformed cells was selectively removed. The Y190 strain is resistant to cycloheximide because of a recessive mutation in the *CYH2* gene. pAS2 contains a wild-type copy of the *CYH2* gene, rendering cells containing pAS-derived plasmids susceptible to cycloheximide. Colonies of doubly transformed cells were streaked onto SC-Leu medium containing 2.5 μg of cycloheximide/ml. Individual colonies were then streaked onto SC-Leu and SC-Leu-Trp plates. Only those colonies that were able to grow on SC-Leu plates and unable to grow on SC-Leu-Trp plates were used further. These cells were then retransformed with a series of pAS2-derived plasmids.

Filter and plate assays for β-galactosidase and His autotrophy. β-Galactosidase (β-Gal) expression in yeast was tested initially by using a filter assay. Cells were streaked onto SC-Leu-Trp medium containing 5% glycerol–2% lactic acid–0.05% glucose and were incubated for 2 to 4 days at 30°C. The colonies were then transferred to a nitrocellulose membrane which was then immersed into liquid nitrogen for at least 10 s. The membrane was placed on a Whatman no. 1 filter paper soaked with 0.3 ml/square inch of Z buffer (60 mM Na_2HPO_4, 40 mM NaH_2PO_4, 10 mM KCl, 1 mM $MgSO_4$, 50 mM β-mercaptoethanol, pH 7.0) containing 1 mg of 5-bromo-4-chloro-3-indolyl-β-D-galactopyranoside (X-Gal; Sigma B-4252)/ml and incubated at 30°C for 2 to 14 h.

A growth assay on plates was used initially to score His autotrophy. Cells were streaked onto SC-His medium containing 5% glycerol–2% lactic acid–0.05% glucose and 25 mM 3-amino-1,2,4-triazole (3-AT; Sigma A8056) and incubated at 30°C for 4 to 8 days.

Quantitation of β-Gal activity. Yeast cells were grown to saturation in liquid SC-Leu-Trp medium including 5% glycerol–2% lactic acid–0.05% glucose and were subcultured in fresh medium with vigorous shaking at 30°C to a density of 3×10^7 to 5×10^7 cells/ml. One milliliter of cells was harvested by centrifugation, resuspended in 200 μl of Z buffer, and permeabilized by vigorous vortexing (6 pulses for 20 s) with 0.15 g of acid-treated glass beads (425 to 600 μm; Sigma G-9268). Cellular debris and glass beads were removed by centrifugation, and 50 μl of the supernatant was diluted in 950 μl of Z buffer. The β-Gal reaction was carried out by adding 200 μl of 4-mg/ml *o*-nitrophenyl β-D-galactopyranoside (ONPG; Sigma N-1127) in 0.1 M potassium phosphate (pH 7) and incubating at 30°C for 30 min. The reaction was stopped by adding 500 μl of 1 M Na_2CO_3 and was further diluted by adding 1 ml of deionized H_2O. Optical density (OD) was measured at a 420-nm wavelength. Total protein was measured in each extract by using the Bio-Rad protein assay dye according to the manufacturer. β-Gal activity units (nanomoles of *o*-nitrophenol per minute per milligram of protein) were calculated as follows: $OD_{420} \cdot v/k \cdot t \cdot p$, where v is the total volume, t is the reaction time (min), p is total protein (mg) in 50 μl of lysate, and k (=0.0045) is the OD of 1-nmol/ml *o*-nitrophenol at a 420-nm wavelength measured by using a 10-mm light path (38).

Quantitative growth assay in SC-His medium. To quantify cell growth in the absence of His, 15 μl of cells derived from the same saturated cultures used for β-Gal quantitation was transferred to 3 ml of SC-His containing 5% glycerol–2% lactic acid–0.05% glucose and 50 mM 3-AT. The cultures were incubated with vigorous shaking at 30°C for 2 to 3 days, depending on the experiment, and OD was measured at a 600-nm wavelength. Adjusted OD_{600} was calculated as follows: OD_{600} of individual transformant − OD_{600} of the control pACT2:pAS2 transformant.

RESULTS

NIb contains two independent NLSs. The NIb protein contains two short, basic regions (Lys3-Arg4-Lys5 and Lys303-Lys304-His305-Lys306), a feature shared by most known NLSs of plants and animals (21, 23, 43, 48). Substitution of these residues abolished nuclear transport of a fusion protein containing NIb and GUS in transgenic plants (37). However, the specific role of these sequences in nuclear transport was not clear, as substitutions of residues at several other positions also eliminated transport activity. To test the hypothesis that these basic regions function as NLSs, fusion proteins containing GUS and NIb residues 1 to 17 or 292 to 316 (Fig. 1A) were expressed and localized in transgenic plants transformed with pGA.G/b.1-17 and pGA.G/b.292-316, respectively. As controls, plants transformed with pGA482 (vector alone), pGA.GUS encoding nonfused GUS, and pGA.GUS/NIb encoding the GUS/NIb fusion protein were analyzed in parallel. Immunoblot analysis was conducted with transgenic leaf extracts using anti-GUS serum. Proteins of approximately 126 kDa and 68 kDa were detected in plants transformed with pGA.GUS/NIb and pGA.GUS, respectively (Fig. 1B, lanes 2 and 3). A consistent feature of all pGA.GUS/NIb-transformed plants was the relatively low level of accumulation of the GUS/NIb fusion protein (Fig. 1B, lane 2), as was noted previously (37). The basis for the low accumulation levels was not investigated further. Immunoreactive proteins that migrated slightly slower than GUS were detected in plants transformed with pGA.G/b.1-17 and pGA.G/b.292-316 (lanes 5 and 6). No immunoreactive proteins were detected in plants transformed with the vector alone (lane 1).

The subcellular localization properties of GUS and GUS fusion proteins were investigated in epidermal cells from leaves of transgenic plants by using the histochemical substrate X-Gluc. No GUS activity was detected in plants transformed with vector alone (Fig. 2). GUS activity was dispersed in the cytoplasm of GUS-expressing cells, whereas the activity in the GUS/NIb-expressing cells was detected predominantly in the nucleus. In cells expressing the GUS/b.1-17 and GUS/b.292-316 proteins, GUS activity was localized primarily to the nucleus, although in some cells a low level of GUS activity was detected in the cytoplasm (Fig. 2). These data indicate that two regions of NIb, comprising residues 1 to 17 and 292 to 316, contain functional NLSs (NLS I and NLS II, respectively).

Amplification and complementation of NIb transport-defective TEV mutants in protoplasts and plants. A mutation resulting in the substitution of Asp-Asp for Lys303-Lys304 (DD mutation) was introduced into the TEV-GUS genome. Mutations resulting in substitutions of Glu-Asp-Glu for Lys3-Arg4-Lys5 (EDE mutation) within NLS I and Val-Asn-Asn for the conserved motif Gly347-Asp348-Asp349 (VNN mutation) were placed in the TEV-GUS genome previously and shown to debilitate RNA amplification (36). The VNN mutant, but not the EDE mutant, was shown to be complemented relatively efficiently by NIb supplied in *trans* by transgenic cells (36). The amplification and complementation properties of the DD mutant in protoplasts and plants were analyzed in parallel with parental TEV-GUS and the EDE and VNN mutants. Protoplasts from vector transgenic or NIb$^+$ transgenic plants were inoculated with transcripts representing each genome, and GUS activity at 24, 48, and 72 h p.i. was measured as a surrogate marker for viral RNA amplification over time. This experiment was repeated three times with protoplasts prepared from independent transgenic plants. Similar to the VNN and EDE mutants, the DD mutant was unable to amplify in vector-transformed protoplasts (Fig. 3, left panels). In NIb$^+$ protoplasts, however, the DD mutant was amplified to a level comparable to that of the VNN mutant (Fig. 3, right panels). At 48 h p.i., GUS activity in DD mutant- and VNN mutant-infected NIb$^+$ cells reached 38.3% ± 6.6% and 24.8% ± 6.0%, respectively, of the level of activity in parental TEV-GUS-infected cells. Activity in the EDE mutant-infected NIb$^+$ cells reached a relative level of only 1.8% ± 0.7% compared to that in parental virus-infected cells. The differential complementation levels of the DD and EDE mutants suggest that, although both NLS I and NLS II overlap with regions essential for NIb

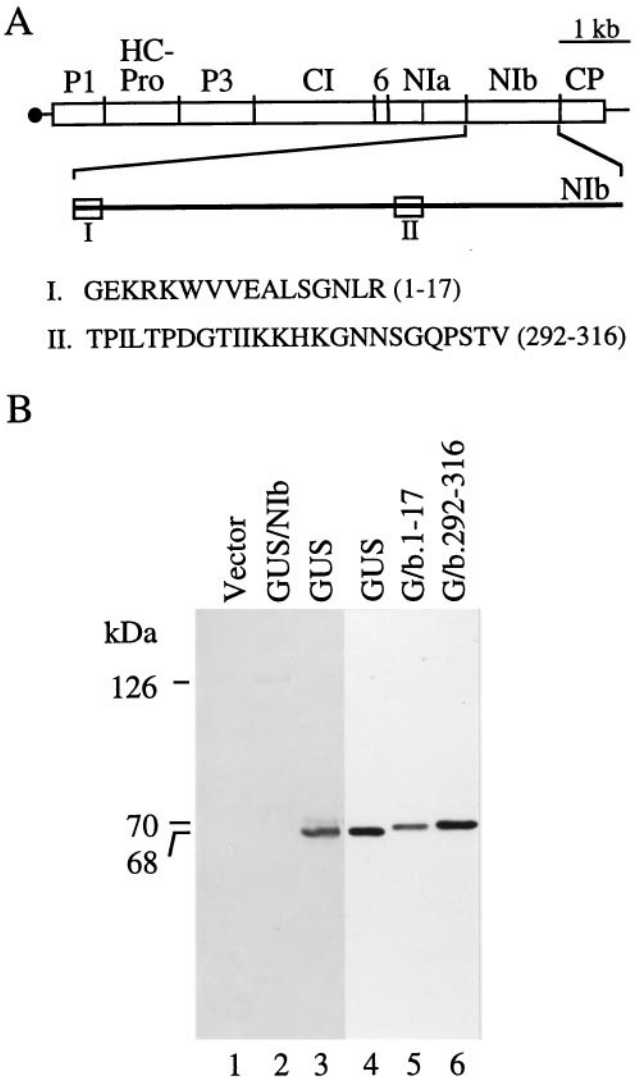

FIG. 1. Genetic map of the TEV genome and immunoblot analysis of transgenic plants. (A) Map of the TEV genome with the coding regions for individual proteins indicated above. Vertical lines indicate positions coding for proteolytic cleavage sites. The region representing NIb is enlarged below the genetic map. The sequences encompassing NLS I (residues 1 to 17) and NLS II (292 to 316) are indicated by the boxes on the enlargement and presented in single-letter code. (B) Total protein was extracted from leaves of transgenic tobacco plants and subjected to sodium dodecyl sulfate-polyacrylamide gel electrophoresis (SDS-PAGE) and immunoblot analysis with anti-GUS serum. Samples in lanes 1 to 3 and lanes 4 to 6 were analyzed in two separate blots, which is why the GUS-containing extract is shown in both lanes 3 and 4. The calculated molecular masses for GUS (68 kDa), GUS/NIb fusion protein (126 kDa), and fusion protein containing GUS and residues 1 to 17 of NIb (G/b.1-17) (70 kDa) are indicated at the left.

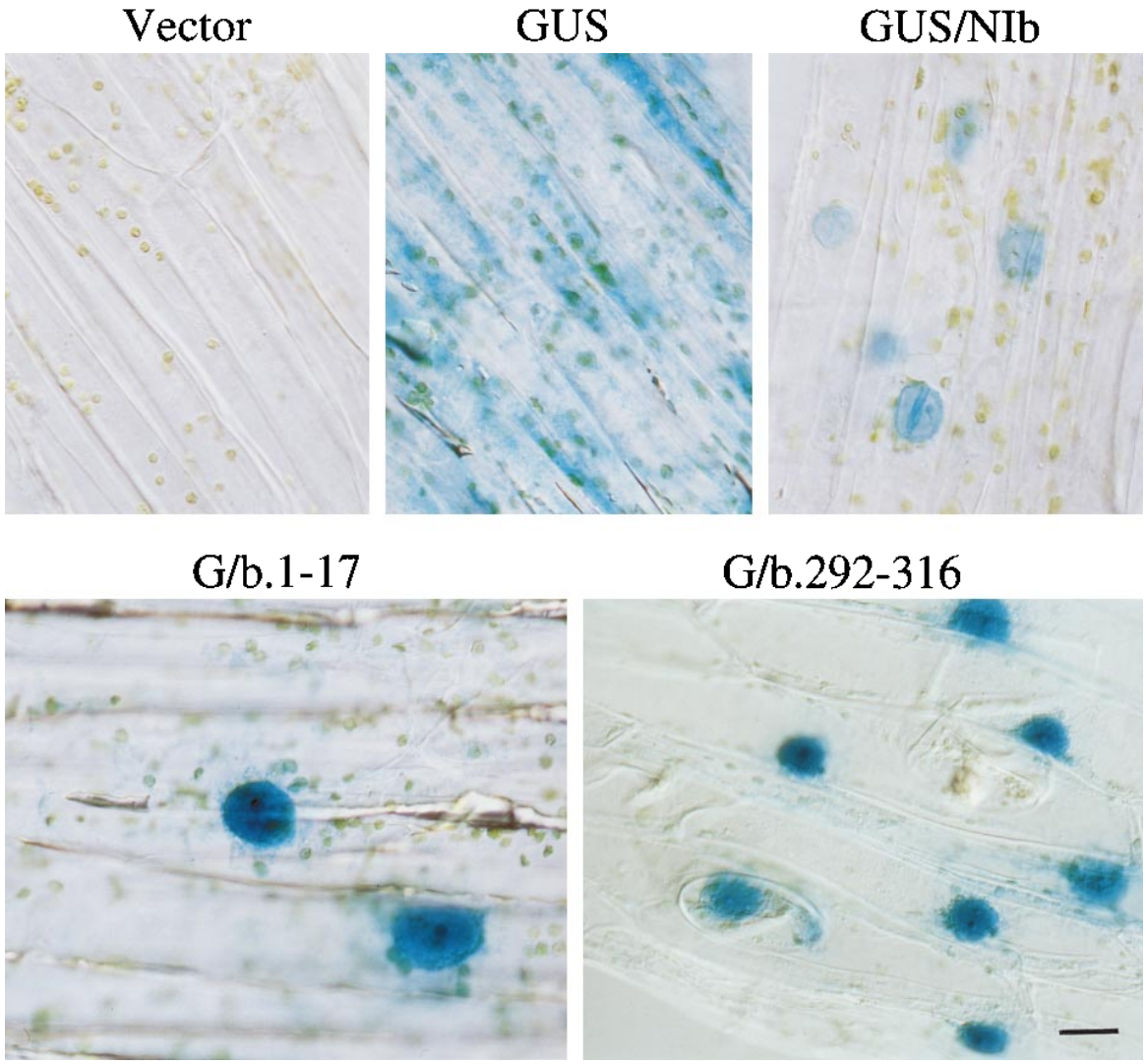

FIG. 2. In situ localization of GUS activity on leaf epidermal cells of transgenic tobacco plants. Plants were transformed with empty vector (Vector) or with plasmids encoding GUS, GUS/NIb fusion protein, or fusion proteins containing GUS and NIb residues 1 to 17 (G/b.1-17) or 292 to 316 (G/b.292-316.) β-Gluc activity was detected by incubation of epidermal cells in the colorimetric substrate X-Gluc. Bar = 20 μm.

activity, the functions disrupted by the NLS mutations may be distinct.

Transgenic NIb$^+$ plants, but not vector-transformed plants, inoculated with the VNN, EDE, and DD mutant transcripts exhibited symptoms similar to those induced by parental TEV-GUS in upper, noninoculated leaves. Extracts from these infected plants were used to inoculate several leaves in each of three vector-transformed and NIb$^+$ transgenic plants, and inoculated leaves were infiltrated with X-Gluc at 3 days p.i. Infection foci (between 50 to 200 per leaf) and systemic symptoms were detected in NIb$^+$ transgenic plants but not in vector-transformed plants (data not shown), confirming that the virus produced in transgenic cells was the result of actual *trans*-complementation rather than reversion or recombination with the transgene.

NIb interacts specifically with NIa. The fact that NIb-defective mutants can be rescued by mature NIb from transgenic cells indicates that this protein can function in *trans*. Recruitment of NIb to replication complexes likely involves interactions with other viral replication proteins, host factors, or viral RNA. To test the hypothesis that NIb interacts with other TEV replication proteins with catalytic functions in genome replication, a combinatorial two-hybrid system was used. Viral proteins were expressed in yeast Y190 cells as fusion proteins containing either GAL4 ACT or DB (17). The nomenclature of each strain provides the code for the TEV or control protein fused to ACT, a colon, and then the code for the protein fused to DB. Protein-protein interaction was assayed by GAL4-mediated activation of *lacZ* and *HIS3* reporter genes. Activation was first tested by a β-Gal filter assay and growth on His-lacking (SC-His) solid medium and then by quantitative β-Gal and His-independent growth assays using liquid cultures. For a positive control, a strain designated S4:S1, which expresses fusion proteins containing the yeast SNF1 and SNF4 proteins and which are known to interact (18), was used. For negative controls, cells transformed with the two parental vectors encoding nonfused ACT and DB (v:v strain) or cells expressing a TEV fusion protein and fusions containing either GUS, SNF1, or SNF4 were used. Most combinations of fusion proteins tested are listed in Tables 1 and 2.

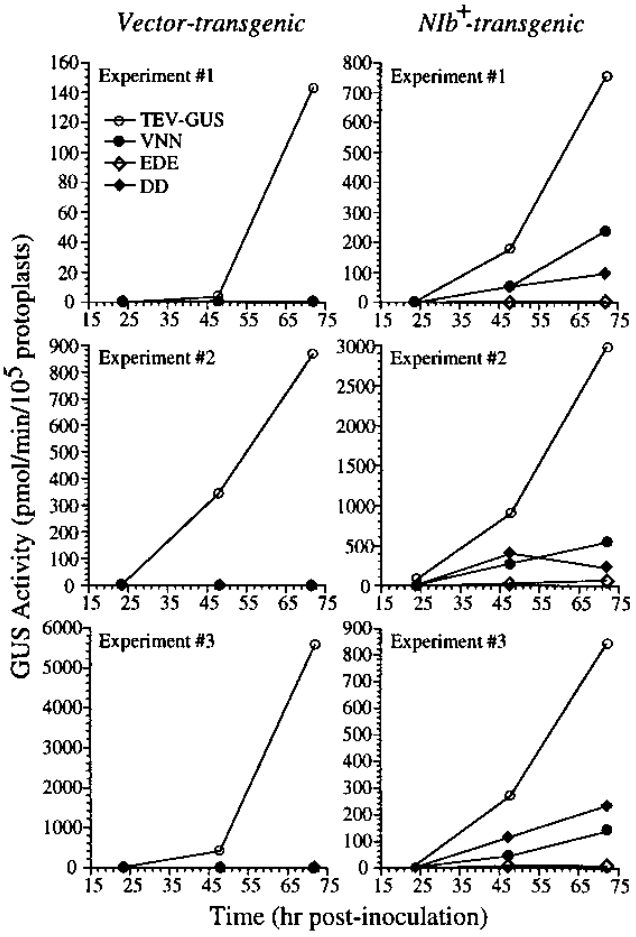

FIG. 3. Complementation of NIb-defective TEV-GUS mutants in NIb$^+$ transgenic protoplasts. Transcripts corresponding to parental TEV-GUS or the VNN, EDE, and DD mutants were used to inoculate vector transgenic (left panels) or NIb$^+$ transgenic (right panels) protoplasts. GUS activity was measured from samples taken at 24, 48, and 72 h p.i. Each datum point represents the mean GUS value from two contemporaneous transfections. Data from three independent experiments with different protoplast preparations are shown. Note that independent protoplast preparations isolated from the same line in the independent experiments often differed in absolute susceptibility but that the relative amplification levels of parental TEV-GUS and each given mutant virus were reproducible.

TABLE 1. Yeast strains, fusion combinations, and β-Gal filter assays

Yeast strain	ACT fusion	DB fusion	β-Gal filter assay[a]
v:v	Vector alone	Vector alone	−
S4:S1	SNF4	SNF1	+++
a:a	NIa	NIa	−
a:b	NIa	NIb	+++
a:CI	NIa	CI	−
a:S1	NIa	SNF1	+/−
a:Δb+b	NIa	NIb (NIb depleted, NIb added back)	+++
a:Δb+G	NIa	GUS (NIb depleted, GUS added back)	−
a:Δb+S1	NIa	SNF1 (NIb depleted, SNF1 added back)	+/−
b:a	NIb	NIa	+++
S4:a	SNF4	NIa	−
CI:a	CI	NIa	−
b:Δa+a	NIb	NIa (NIa depleted, NIa added back)	+++
b:Δa+b	NIb	NIb (NIa depleted, NIb added back)	−
b:Δa+CI	NIb	CI (NIa depleted, CI added back)	ND
b:Δa+S1	NIb	SNF1 (NIa depleted, SNF1 added back)	+/−
b:Δa+G	NIb	GUS (NIb depleted, GUS added back)	−
CI:b	CI	NIb	−
CI:G	CI	GUS	−
G:CI	GUS	CI	−

[a] Colorimetric β-Gal filter assays were conducted by using at least three independent transformants of each yeast strain. Reactions were scored as follows: −, no visible reaction after overnight incubation; +/−, weak, inconsistent reaction that required overnight development; +++, strong reaction that developed within 30 min; ND, not determined.

In β-Gal filter assays, all strains expressing both NIa and NIb (a:b or b:a) turned dark blue within 30 min, as did the S4:S1 positive control strain (Table 1 and Fig. 4B). The a:S1, S4:a, and v:v strains failed to exhibit activity. Similarly, the a:b, b:a, and S4:S1 control strains grew on SC-His solid medium, whereas growth of the a:S1, S4:a, and v:v strains was dependent on exogenous His (Fig. 4C). To confirm that β-Gal activation and His autotrophy of the a:b and b:a strains were the result of a specific interaction between NIa and NIb, the pAS2-derived plasmid was depleted from both strains. Strains in which the pAS2-based plasmid was depleted were given either a Δa or Δb designation, depending on the specific plasmid depleted. These strains were then retransformed with a series of pAS2-derived plasmids encoding DB fusions with SNF1, GUS, NIa, or NIb. Only the retransformed strains containing both NIa and NIb fusions (a:Δb+b and b:Δa+a) exhibited β-Gal activity in the filter assay and growth on SC-His plates (Table 1 and Fig. 4B and C).

Quantitative assays for β-Gal activity and His autotrophy were conducted with this initial series of strains, as well as with all subsequent series of strains, using liquid cultures. At least three independent double transformants were tested for most two-hybrid combinations. Evidence for a positive interaction was considered good if relatively high β-Gal activity and growth in SC-His medium were evident for each of the three individual transformants. Cells expressing both NIa and NIb hybrid proteins (a:b, b:a, a:Δb+b, and b:Δa+a), as well as the control SNF4 and SNF1 hybrid proteins (S4:S1), expressed relatively high levels of β-Gal activity (Fig. 5A) and grew well in SC-His medium (Fig. 5B). β-Gal activity was approximately threefold higher on average in cells expressing NIa fused to ACT and NIb fused to DB than in cells expressing the reciprocal hybrids. Although β-Gal activity in each transformant containing the NIa and NIb fusion proteins was consistently high, some variation was observed. Generally, differences between individual transformants were less than twofold in a given experiment, but in a few cases this variation was as high as fourfold. Combinations involving non-TEV proteins and NIa or NIb (a:S1, a:Δb+G, a:Δb+S1, S4:a, b:Δa+S1, and b:Δa+G) yielded β-Gal activity that was 100- to 1,000-fold lower than the corresponding a:b or b:a strains (Fig. 5A), and growth in SC-His medium was poor (Fig. 5B). Similarly, in strains expressing fusions to detect self-interactions of NIa and NIb (a:a and b:Δa+b), no β-Gal activity above background was detected, and growth in SC-His was poor (Table 1 and Fig. 5).

The physiological role for the CI helicase in TEV genome replication is not clear, but it presumably interacts with viral RNA and other replication proteins during initiation and/or

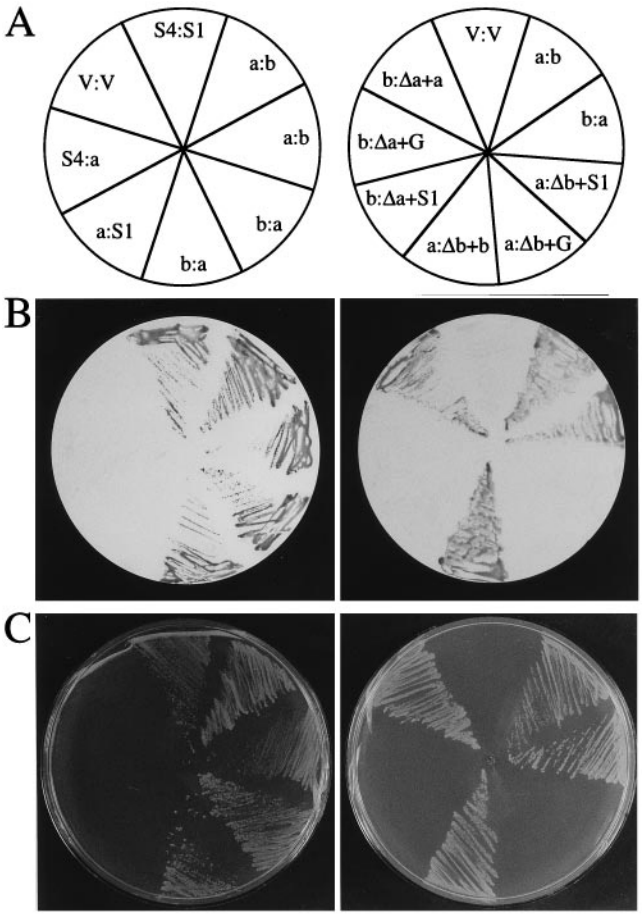

FIG. 4. β-Gal filter assay and plate-based His-independent growth assay of yeast in the two-hybrid system. (A) Diagram of arrangement of yeast strains on each set of plates. (B) β-Gal assay on nitrocellulose filters with the colorimetric substrate X-Gal. (C) Growth of yeast on His-SC medium. Note that each yeast strain that exhibited β-Gal activity also displayed His-independent growth.

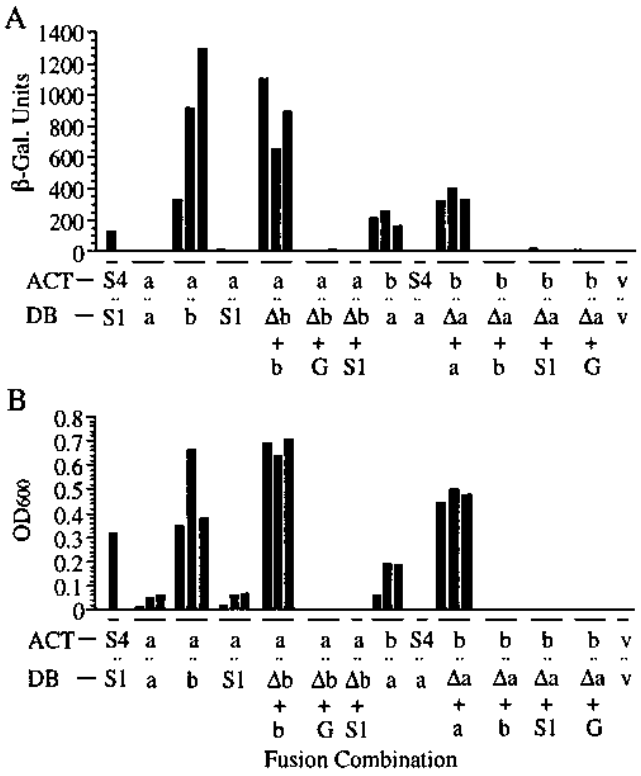

FIG. 5. β-Gal and His-independent growth assays of yeast containing two-hybrid combinations of NIa, NIb, and control proteins. The results of quantitative β-Gal (nanomoles of *o*-nitrophenol per minute per milligram of total protein) assays using extracts from liquid cultures (A) and growth (OD_{600}) in SC-His medium (B) are shown. Three independently transformed yeast strains containing most two-hybrid combinations were tested and plotted on each graph. The codes for each protein fused to GAL4 ACT and DB are as follows: a, NIa; b, NIb; G, GUS; S1, SNF1; S4, SNF4; v, no protein fused to either ACT or DB. Strains with a Δa or Δb designation were depleted of the plasmid encoding the DB fusion protein, and then retransformed with a plasmid encoding the same or a different DB fusion protein.

chain elongation reactions (47). The ability of the CI helicase to interact with NIa or NIb in the two-hybrid assay was tested. Reciprocal combinations were tested between NIa and CI (a:CI and CI:a) and between NIb and CI (b:CI and CI:b). Also, control strains expressing CI and GUS (CI:G and G:CI) were tested. In both the plate and liquid culture-based assays, neither β-Gal activity nor His-independent growth were detected in strains expressing any of these CI fusion combinations (Table 1 and data not shown).

Domains involved in the NIa-NIb interaction. To identify regions or domains within NIb that are necessary for the NIa-NIb interaction, a series of five pAS2-derived plasmids with deletions collectively spanning the entire NIb sequence was generated and introduced into yeast cells known to contain active NIa fusion protein, resulting in strains a:bΔ1, a:bΔ2, a:bΔ3, a:bΔ4, and a:bΔ5 (Table 2). The proteins encoded by the bΔ1 and bΔ5 mutants contained deletions of either the N-terminal 141 or C-terminal 100 residues, respectively. These sequences represent the least conserved regions in comparison with other RNA polymerases encoded by picornavirus-like supergroup members (30). The bΔ2, bΔ3, and bΔ4 mutant proteins lacked the regions containing or immediately flanking the highly conserved polymerase core region (30, 31). No β-Gal activity above background and poor or no growth in SC-His were detected with these strains (Table 2 and Fig. 6). In the strains containing bΔ1, bΔ2, bΔ3, and bΔ4, the lack of interaction with NIa was not due to instability of the truncated protein, as immunoblot analysis revealed that each strain accumulated an NIb-fusion protein to approximately the same level as wild-type NIb (Fig. 7). In the strain containing the bΔ5 variant, however, no anti-NIb-reactive protein was detected (data not shown). Using this deletion series, we were unable to identify within NIb a functionally discrete domain for interaction with NIa.

The VNN, EDE, and DD mutations were introduced into the DB-NIb-encoding plasmid. The modified plasmids were introduced into yeast cells expressing active ACT-NIa fusion protein, resulting in the a:VNN, a:EDE, and a:DD strains. β-Gal activity and growth in SC-His medium were high, or even enhanced, in the a:EDE strain (Table 2 and Fig. 6). In contrast, β-Gal activity and His-independent growth were relatively low in the a:VNN strain and near background levels in the a:DD strain. In multiple immunoblot experiments, one of which is shown in Fig. 7, the relative signal intensities of wild-type and mutant NIb fusion proteins were generally comparable, indicating that the low interaction activity in the a:VNN and a:DD strains was not due to low levels of fusion protein accumulation. These data suggest that the GDD motif and the NLS II sequence contribute either directly or indirectly to the

TABLE 2. Yeast strains, fusion combinations, and β-Gal filter assays

Yeast strain	ACT fusion[a]	DB fusion	β-Gal filter assay[a]
a:bΔ1	NIa	NIb, aa 1–141 deleted[b]	−
a:bΔ2	NIa	NIb, aa 142–243 deleted	−
a:bΔ3	NIa	NIb, aa 244–354 deleted	−
a:bΔ4	NIa	NIb, aa 355–412 deleted	−
a:bΔ5	NIa	NIb, aa 413–512 deleted	+/−
a:VNN	NIa	NIb, VNN mutation	+
a:EDE	NIa	NIb, EDE mutation	+++
a:DD	NIa	NIb, DD mutation	−
VPg:b	NIa VPg domain (aa 1–188)	NIb	−
b:VPg	NIb	NIa VPg domain (aa 1–188)	−
Pro:b	NIa Pro domain (aa 189–430)	NIb	+
Pro:EDE	NIa Pro domain (aa 189–430)	NIb with EDE mutation	+++
Pro:DD	NIa Pro domain (aa 189–430)	NIb with DD mutation	−
Pro:VNN	NIa Pro domain (aa 189–430)	NIb with VNN mutation	+
Pro:a	NIa Pro domain (aa 189–430)	NIa	−
Pro:VPg	NIa Pro domain (aa 189–430)	NIa VPg domain (aa 1–188)	−
Pro:Pro	NIa Pro domain (aa 189–430)	NIa Pro domain (aa 189–430)	−
Pro:CI	NIa Pro domain (aa 189–430)	CI	−
Pro:G	NIa Pro domain (aa 189–430)	GUS	−
Pro:v	NIa Pro domain (aa 189–430)	Vector	−
b:Pro	NIb	NIa Pro domain (aa 189–430)	+

[a] Colorimetric β-Gal filter assays were conducted by using at least three independent transformants of each yeast strain. Reactions were scored as follows: −, no visible reaction after overnight incubation; +/−, weak, inconsistent reaction that required development overnight; +, weak, but consistent, reaction that required several hours' or overnight development; +++, strong reaction that developed within minutes.

[b] aa, amino acid.

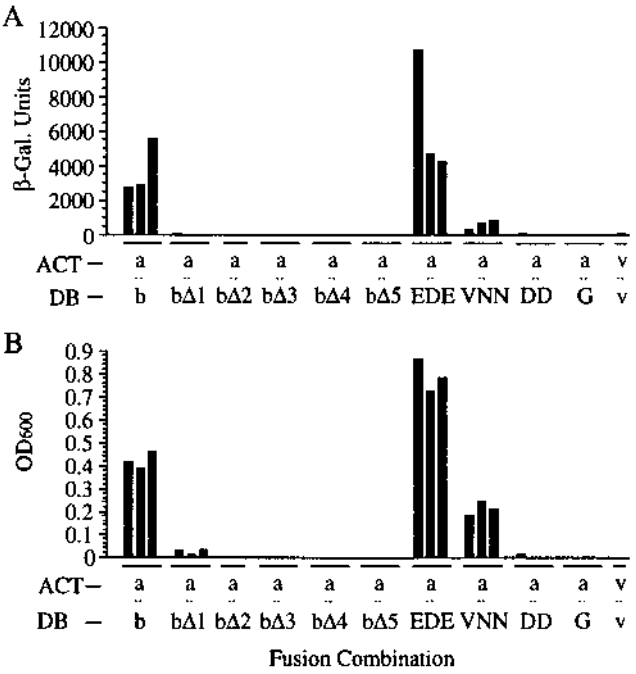

FIG. 6. β-Gal and His-independent growth assays of yeast containing two-hybrid combinations of NIa, wild-type, and mutant forms of NIb, and control proteins. The results of quantitative β-Gal (nanomoles of *o*-nitrophenol per minute per milligram of total protein) assays using extracts from liquid cultures (A) and growth (OD_{600}) in SC-His medium (B) are shown. Three independently transformed yeast strains containing each two-hybrid combination were tested and plotted on each graph, except for the a:bΔ1 strain in which only two transformants were tested. The codes for each protein fused to GAL4 ACT and DB are as follows: a, NIa; b, NIb; G, GUS; bΔ1, bΔ2, bΔ3, bΔ4, bΔ5, EDE, VNN, and DD, mutant forms of NIb as described in the text; v, no protein fused to either ACT or DB.

interaction between NIa and NIb, but that the NLS I region is dispensable for the interaction.

To determine whether the VPg or Pro domain of NIa is involved in the NIa-NIb interaction, two-hybrid combinations with VPg (residues 1 to 188) and Pro (residues 189 to 430) fusions were tested. Each yeast strain with VPg and Pro fusion constructs was shown by PCR analysis to contain plasmid DNA with an intact insert. However, immunoblot analysis with NIa polyclonal antibody (44), or with VPg or Pro domain monoclonal antibodies (51), revealed that each protein accumulated to either very low or nondetectable levels. The ACT-VPg fusion was expressed in combination with DB fusions containing NIb (VPg:b), NIa (VPg:a), the VPg (VPg:VPg), or Pro (VPg:Pro) domains, CI (VPg:CI), or a negative control (VPg:GUS). None of the strains containing combinations involving the VPg domain yielded β-Gal activity or grew in SC-His medium (Table 2 and data not shown). Similar results were obtained when each reciprocal combination involving DB-VPg was tested (Table 2 and data not shown).

In contrast, the Pro domain clearly interacted with NIb. The Pro:b and b:Pro strains yielded moderate levels of β-Gal activity and grew well in SC-His medium (Table 2 and Fig. 8), although β-Gal and His-independent growth activities were lower than with a:b strains. Importantly, the effects of the NIb EDE, VNN, and DD mutations on the Pro-NIb interaction were similar to those measured with the a:b combination. The EDE mutation had no debilitating effects on β-Gal activity or His-independent growth, whereas the VNN and DD mutations dramatically reduced or eliminated both reporter activities (Fig. 8). No evidence of an interaction was observed with fusion combinations involving the Pro domain and NIa (Pro:a), the VPg (Pro:VPg) or Pro (Pro:Pro) domains, CI (Pro:CI), or negative controls (Table 2 and Fig. 8). These results strongly suggest that the Pro domain is a primary determinant within NIa involved in the NIa-NIb interaction.

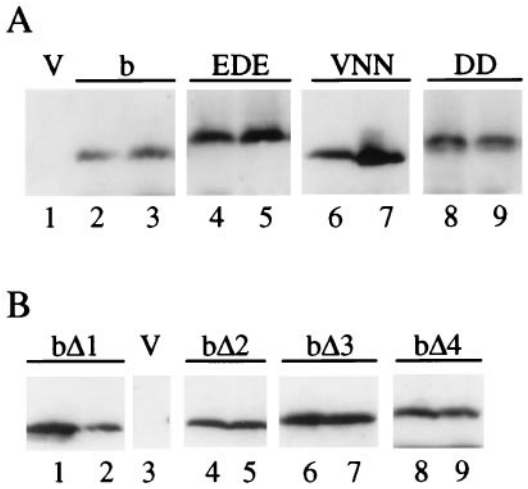

FIG. 7. Immunoblot analysis of DB fusion proteins containing wild-type NIb or mutant NIb derivatives from yeast. Two independently transformed yeast strains containing each DB-NIb fusion protein and ACT-NIa fusion protein were analyzed in parallel using equivalent amounts of extract. Blotted proteins were reacted with an anti-NIb monoclonal antibody cocktail (51), and immunoreactive proteins were detected by using a chemiluminescence system. (A) Extracts were prepared from vector-transformed yeast (lane 1), or yeast expressing fusion proteins containing wild-type NIb (lanes 2 and 3), EDE NIb mutant (lanes 4 and 5), VNN NIb mutant (lanes 6 and 7), and DD NIb mutant (lanes 8 and 9). The EDE and DD mutant fusion proteins consistently migrated more slowly than the wild-type fusion protein. (B) Extracts were prepared from yeast expressing the bΔ1 (lanes 1 and 2), bΔ2 (lanes 4 and 5), bΔ3 (lanes 6 and 7), and bΔ4 (lanes 8 and 9) DB-NIb deletion variants and from vector-transformed yeast (lane 3). The data shown in panels A and B were from two SDS-PAGE gels processed simultaneously with the same antibody concentration, incubation conditions, and exposure times. Only the regions of the immunoblots showing the fusion proteins are presented.

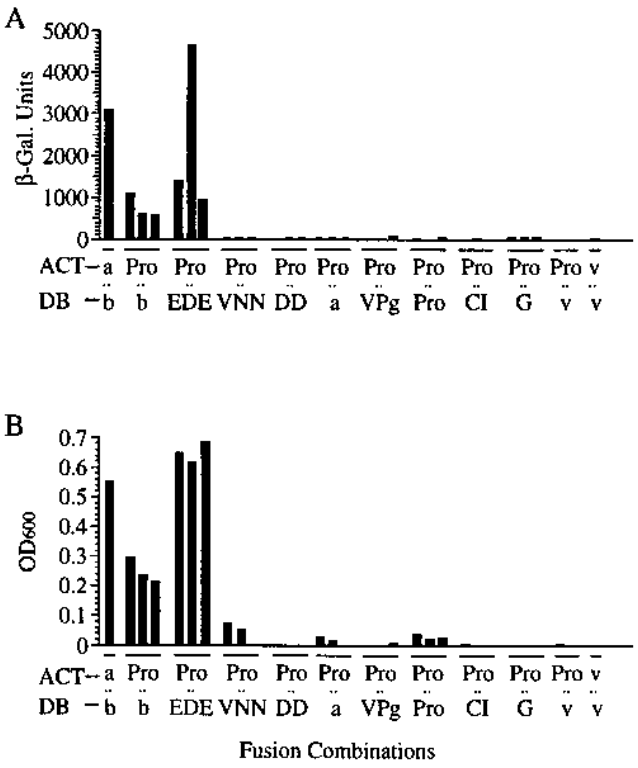

FIG. 8. β-Gal and His-independent growth assays of yeast containing two-hybrid combinations with the Pro domain of NIa. The results of quantitative β-Gal (nanomoles of *o*-nitrophenol per minute per milligram of total protein) assays using extracts from liquid cultures (A) and growth (OD_{600}) in SC-His medium (B) are shown. Three independently transformed yeast strains containing each two-hybrid combination were tested and plotted on each graph, except for the a:b, Pro:v, and v:v strains. The codes for each protein fused to GAL4 ACT and DB are as follows: a, NIa; b, NIb; EDE, VNN, and DD, mutant forms of NIb as described in the text; G, GUS; VPg, VPg domain of NIa; Pro, proteinase domain of NIa; v, no protein fused to either ACT or DB.

DISCUSSION

Nuclear transport signals of NIb. Our previous efforts to define the NLS(s) within the full-length NIb were not successful due to the high sensitivity of transport to sequence alterations at numerous positions (37). However, two regions in NIb, including residues 3 to 5 and 303 to 306, were suspected previously to be possible NLSs based on their Arg- and Lys-rich sequences. Substitutions of these residues within the GUS/NIb fusion protein abolished nuclear translocation (37). In the present study, NLS functions of the NIb 1 to 17 and 292 to 316 amino acid segments, which include the basic residues at positions 3 to 5 and 303 to 306, respectively, were demonstrated when each segment was fused to the C terminus of GUS independently from the remainder of NIb.

Although the 1 to 17 and 292 to 316 amino acid segments of NIb by themselves function independently as NLSs, their activities within NIb appear to depend heavily on the structural integrity of the protein. Such structure-dependent NLS activity has been detected in other systems. For example, although the region containing the carboxyl-terminal 28 residues of herpes simplex virus ICP8 contains an independent NLS, introduction of modifications at other sites impedes nuclear translocation (19). The susceptibility of translocation to structural modifications raises the possibility that control of NIb nuclear transport might be achieved by conformational changes.

It should be stressed that although mutations affecting the basic residues within the NLSs rendered TEV-GUS nonviable, a requirement for NIb in the nucleus has not been demonstrated. The sequences altered in the EDE and DD mutants may be necessary for NIb functions other than nuclear translocation. The complementation data are consistent with this idea. If the NIb variants encoded by these mutants were defective only in nuclear translocation, they should have been complemented to comparable levels in NIb^+ cells. The fact that the DD mutant was complemented to a level 21-fold greater than the EDE mutant suggests that distinct functions were affected by each mutation. Alternatively, the EDE and DD mutations may have affected the same NIb replication function, but the EDE mutant encoded a NIb protein with dominant-negative properties that inhibited the complementing activity of transgenic NIb.

Interaction between NIa and NIb. The finding that TEV mutants containing replication-debilitating point mutations affecting NIb, or lacking the NIb sequence altogether, could be complemented in transgenic cells indicated that NIb is a *trans*-active protein (36). A *trans*-active protein must be recruited to active replication complexes by interactions with other replication factors or templates. Among the three TEV proteins with known enzymatic functions in RNA replication, i.e., the NIa, NIb, and CI proteins, an interaction was detected only between NIa and NIb in the yeast two-hybrid system. Hong et al. (26) have also demonstrated that NIa and NIb encoded by the related potyvirus, tobacco vein mottling virus, physically interact. Because deletions throughout the entire NIb molecule abolished the NIa-NIb interaction, a specific interaction domain within NIb was not identified. The interaction function of NIb may depend on multiple regions within the NIb protein

or it may involve a stringent structural requirement throughout the entire protein as has been suggested for the nuclear transport function. This differs from protein-protein interactions of some other positive-strand RNA virus polymerases. In the case of brome mosaic virus 2a polymerase, an interaction with the 1a replication protein is mediated by a discrete N-terminal domain (27, 28). Within NIa, however, the picornavirus 3C-like Pro region was identified as an NIb-interacting domain. Two lines of evidence support this conclusion. First, the Pro domain alone interacted with NIb in the yeast system. And second, the effects of three NIb clustered point mutations (EDE, DD, and VNN) on the NIa-NIb and Pro-NIb interactions were similar. While these data strongly implicate the Pro domain as the interacting region within NIa, they do not exclude a possible stabilizing or secondary effect of the VPg domain on the interaction. Furthermore, although no interaction between the VPg domain and NIb was detected, it is possible that these proteins do interact in virus-infected cells but that the yeast system was inadequate or insufficiently sensitive. Failure to detect an interaction in the two-hybrid system could be due to inactivation by GAL4 ACT or DB or to levels of accumulation of fusion protein below a critical threshold, as well as to an inherent inability of two proteins to interact.

Neither self-interaction of NIb nor interactions between the CI helicase and either NIa or NIb were detected in the yeast two-hybrid system. The lack of an observable self-interaction of NIb is in contrast to the poliovirus $3D^{pol}$. Active $3D^{pol}$ functionally oligomerizes in vitro, prompting the conclusion that it may act as a cooperative RNA-binding factor during poliovirus RNA synthesis (41). The lack of detection of NIb self-interaction may indicate functional differences between the picornavirus and potyvirus polymerases. Alternatively, failure to detect NIb-NIb interaction may have been due to interfering effects of the GAL4 domains in one or both fusion proteins or to another suboptimal experimental condition. Several possibilities of explaining the inability to detect interactions involving the CI helicase, which is known to be required for RNA replication (29), should be considered. The CI protein may not physically interact directly with either NIa or NIb. The recruitment of CI protein to initiating or elongating replication complexes may involve interactions with RNA or with proteins other than those analyzed here. The recruitment of CI helicase to replication complexes might also be mediated through interactions involving CI polyproteins, or other replication-associated polyproteins, none of which were tested. In addition, failure to detect interactions might also have been due to one or more of the limitations of the yeast two-hybrid assay as discussed above.

The effects of EDE, DD, and VNN mutations on the NIa-NIb interaction could explain some of the genetic properties of the NIb polymerase. The VNN and DD mutations resulted in NIb variants that interacted poorly with NIa, whereas the EDE mutation had no inhibitory effect. In transgenic complementation experiments with mutant TEV-GUS genomes, the VNN and DD mutants were rescued relatively efficiently by NIb in *trans*, whereas the EDE mutant was rescued poorly. This difference could have been due to an interfering effect of the defective NIb encoded by the EDE mutant. The EDE variant protein may interact tightly with NIa in infected transgenic cells, thus excluding access by functional NIb. The DD and VNN mutant proteins, on the other hand, may be incapable of interacting with NIa and, therefore, might not interfere with the complementing activity of the transgenic protein. In this sense, the EDE protein may display the properties of a dominant-negative molecule. If the complementation data are explained by interference effects of the mutant NIb molecules, then such a result may indicate that NIa-NIb interaction represents an important step in the TEV RNA replication process. This hypothesis could be tested further by analyzing the effects of additional NIb mutations on genome replication, complementation, and protein-protein interaction with NIa.

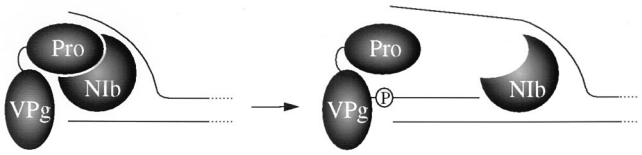

FIG. 9. Model for the interaction of NIa and NIb during initiation of positive-strand RNA synthesis. An interaction is proposed between NIb and the Pro domain of NIa to recruit NIb to active replication complexes. Initiation of RNA synthesis may involve a priming mechanism by the VPg domain of NIa, resulting in covalent linkage of NIa or VPg domain to the 5′-phosphate group of the nascent RNA.

How might the interactions described here relate to replication of the TEV genome? The NIb polymerase may be recruited to initiation complexes through protein-protein interactions with the Pro domain of intact NIa (Fig. 9). The NIa protein itself may be anchored to membranes in the form of a 6K/NIa polyprotein, or a larger polyprotein containing 6K/NIa, as proposed previously (45, 46). How an NIa-NIb complex might be associated with viral RNA or with other replication proteins is not yet known. Initiation of RNA synthesis may be stimulated by a priming mechanism involving the VPg domain of NIa, as proposed for picornaviruses (22, 52, 53). Interestingly, the proposed involvement of an NIa-NIb complex in potyviral replication bears functional similarity to the involvement of the $3C^{pro}$-$3D^{pol}$ polyprotein (3CD) in picornaviral RNA synthesis. Biochemical and genetic evidence support a model in which 3CD, in association with the 3AB VPg precursor polyprotein, binds specifically to an "open" double-stranded RNA template during positive-strand RNA synthesis (3, 4, 24, 39, 42, 54, 55). Internal proteolytic cleavage by 3CD releases 3D to catalyze RNA synthesis (39). In effect, the potyviral and picornaviral models converge on the recruitment of active polymerase through interaction with the 3C or 3C-like (NIa) Pro domain; in picornaviruses this interaction is mediated through a covalent bond within a polyprotein, while in the potyviruses this interaction is through noncovalent protein-protein contacts.

ACKNOWLEDGMENTS

We thank Stephen Elledge for generously providing the yeast two-hybrid system, Erica Graff for excellent assistance in preparing yeast media, Tom McKnight for his gift of anti-GUS serum, Bill Dougherty for monoclonal NIb antibodies, and Tim Hall for kindly allowing us access to his spectrophotometer. We also thank Stephen Johnston, Pam Cascone, Cheng Kao, and Rene Quadt for helpful discussions on yeast techniques.

This research was supported by the National Institutes of Health (AI27832) and the National Science Foundation (IBN-9158559).

REFERENCES

1. **Allison, R., R. E. Johnston, and W. G. Dougherty.** 1986. The nucleotide sequence of the coding region of tobacco etch virus genomic RNA: evidence for the synthesis of a single polyprotein. Virology **154:**9–20.
2. **An, G.** 1987. Binary Ti vectors for plant transformation and promoter analysis. Methods Enzymol. **153:**293–305.
3. **Andino, R., G. E. Rieckhof, P. L. Achacoso, and D. Baltimore.** 1993. Poliovirus RNA synthesis utilizes an RNP complex formed around the 5′-end of viral RNA. EMBO J. **12:**3587–3598.
4. **Andino, R., G. E. Rieckhof, and D. Baltimore.** 1990. A functional ribonucleoprotein complex forms around the 5′ end of poliovirus RNA. Cell **63:**369–380.

5. **Baunoch, D., P. Das, and V. Hari.** 1988. Intracellular localization of TEV capsid and inclusion proteins by immunogold labeling. J. Ultrastruct. Mol. Struct. Res. **99:**203–212.
6. **Carrington, J. C., S. M. Cary, and W. G. Dougherty.** 1988. Mutational analysis of tobacco etch virus polyprotein processing: *cis* and *trans* proteolytic activities of polyproteins containing the 49-kilodalton proteinase. J. Virol. **62:**2313–2320.
7. **Carrington, J. C., and W. G. Dougherty.** 1987. Processing of the tobacco etch virus 49K protease requires autoproteolysis. Virology **160:**355–362.
8. **Carrington, J. C., and W. G. Dougherty.** 1987. Small nuclear inclusion protein encoded by a plant potyvirus genome is a protease. J. Virol. **61:**2540–2548.
9. **Carrington, J. C., and D. D. Freed.** 1990. Cap-independent enhancement of translation by a plant potyvirus 5′ nontranslated region. J. Virol. **64:**1590–1597.
10. **Carrington, J. C., D. D. Freed, and A. J. Leinicke.** 1991. Bipartite signal sequence mediates nuclear translocation of the plant potyviral NIa protein. Plant Cell **3:**953–962.
11. **Carrington, J. C., R. Haldeman, V. V. Dolja, and M. A. Restrepo-Hartwig.** 1993. Internal cleavage and *trans*-proteolytic activities of the VPg-proteinase (NIa) of tobacco etch potyvirus in vivo. J. Virol. **67:**6995–7000.
12. **Dolja, V. V., R. Haldeman, N. L. Robertson, W. G. Dougherty, and J. C. Carrington.** 1994. Distinct functions of capsid protein in assembly and movement of tobacco etch potyvirus in plants. EMBO J. **13:**1482–1491.
13. **Dolja, V. V., H. J. McBride, and J. C. Carrington.** 1992. Tagging of plant potyvirus replication and movement by insertion of β-glucuronidase into the viral polyprotein. Proc. Natl. Acad. Sci. USA **89:**10208–10212.
14. **Domier, L. L., J. G. Shaw, and R. E. Rhoads.** 1987. Potyviral proteins share amino acid sequence homology with picorna-, como-, and caulimoviral proteins. Virology **158:**20–27.
15. **Dougherty, W. G., and T. D. Parks.** 1991. Post-translational processing of the tobacco etch virus 49-kDa small nuclear inclusion polyprotein: identification of an internal cleavage site and delimitation of VPg and proteinase domains. Virology **183:**449–456.
16. **Dougherty, W. G., and B. L. Semler.** 1993. Expression of virus-encoded proteinases: functional and structural similarities with cellular enzymes. Microbiol. Rev. **57:**781–822.
17. **Durfee, T., K. Becherer, P. L. Chen, S. H. Yeh, Y. Yang, A. E. Kilburn, W. H. Lee, and S. J. Elledge.** 1993. The retinoblastoma protein associates with the protein phosphatase type 1 catalytic subunit. Genes Dev. **7:**555–569.
18. **Fields, S., and O. K. Song.** 1989. A novel genetic system to detect protein-protein interactions. Nature (London) **340:**245–246.
19. **Gao, M., and D. Knipe.** 1992. Distal protein sequences can affect the function of a nuclear localization signal. Mol. Cell. Biol. **12:**1330–1339.
20. **García, J. A., J. L. Riechmann, and S. Laín.** 1989. Proteolytic activity of the plum pox potyvirus NIa-like protein in *Escherichia coli*. Virology **170:**362–369.
21. **Garcia-Bustos, J., J. Heitman, and M. N. Hall.** 1991. Nuclear protein localization. Biochim. Biophys. Acta **1071:**83–101.
22. **Giachetti, C., and B. L. Semler.** 1991. Role of a viral membrane polypeptide in strand-specific initiation of poliovirus RNA synthesis. J. Virol. **65:**2647–2654.
23. **Görlich, D., and I. W. Mattaj.** 1996. Nucleocytoplasmic transport. Science **271:**1513–1518.
24. **Harris, K. S., W. Xiang, L. Alexander, W. S. Lane, A. V. Paul, and E. Wimmer.** 1994. Interaction of poliovirus polypeptide $3CD^{pro}$ with the 5′ and 3′ termini of the poliovirus genome: identification of viral and cellular cofactors needed for efficient binding. J. Biol. Chem. **269:**27004–27014.
25. **Hellmann, G. M., J. G. Shaw, and R. E. Rhoads.** 1988. *In vitro* analysis of tobacco vein mottling virus NIa cistron: evidence for a virus-encoded protease. Virology **163:**554–562.
26. **Hong, Y., K. Levay, J. F. Murphy, P. G. Klein, J. G. Shaw, and A. G. Hunt.** 1995. The potyvirus polymerase interacts with the viral coat protein and VPg in yeast cells. Virology **214:**159–166.
27. **Kao, C. C., and P. Ahlquist.** 1992. Identification of the domains required for direct interaction of the helicase-like and polymerase-like RNA replication proteins of brome mosaic virus. J. Virol. **66:**7293–7302.
28. **Kao, C. C., R. Quadt, R. P. Hershberger, and P. Ahlquist.** 1992. Brome mosaic virus RNA replication proteins 1a and 2a form a complex in vitro. J. Virol. **66:**6322–6329.
29. **Klein, P. G., R. R. Klein, E. Rodríguez-Cerezo, A. G. Hunt, and J. G. Shaw.** 1994. Mutational analysis of the tobacco vein mottling virus genome. Virology **204:**759–769.
30. **Koonin, E. V.** 1991. The phylogeny of RNA-dependent RNA polymerases of positive-strand RNA viruses. J. Gen. Virol. **72:**2197–2206.
31. **Koonin, E. V., G. H. Choi, D. L. Nuss, R. Shapira, and J. C. Carrington.** 1991. Evidence for common ancestry of a chestnut blight hypovirulence-associated double-stranded RNA and a group of positive-strand RNA plant viruses. Proc. Natl. Acad. Sci. USA **88:**10647–10651.
32. **Koonin, E. V., and V. V. Dolja.** 1993. Evolution and taxonomy of positive-strand RNA viruses: implications of comparative analysis of amino acid sequences. Crit. Rev. Biochem. Mol. Biol. **28:**375–430.
33. **Kunkel, T. A., J. D. Roberts, and R. Zakour.** 1987. Rapid and efficient site-specific mutagenesis without phenotypic selection. Methods Enzymol. **154:**367–382.
34. **Laín, S., M. T. Martín, J. L. Riechmann, and J. A. García.** 1991. Novel catalytic activity associated with positive-strand RNA virus infection: nucleic acid-stimulated ATPase activity of the plum pox potyvirus helicase protein. J. Virol. **65:**1–6.
35. **Laín, S., J. L. Riechmann, and J. A. García.** 1990. RNA helicase: a novel activity associated with a protein encoded by a positive-strand RNA virus. Nucleic Acids Res. **18:**7003–7006.
36. **Li, X. H., and J. C. Carrington.** 1995. Complementation of tobacco etch potyvirus mutants by active RNA polymerase expressed in transgenic cells. Proc. Natl. Acad. Sci. USA **92:**457–461.
37. **Li, X. H., and J. C. Carrington.** 1993. Nuclear transport of tobacco etch potyviral RNA-dependent RNA polymerase is highly sensitive to sequence alterations. Virology **193:**951–958.
38. **Miller, J. H.** 1972. Experiments in molecular genetics. Cold Spring Harbor Laboratory, Cold Spring Harbor, N.Y.
39. **Molla, A., K. S. Harris, A. V. Paul, S. H. Shin, J. Mugavero, and E. Wimmer.** 1994. Stimulation of poliovirus proteinase $3C^{pro}$-related proteolysis by the genome-linked protein VPg and its precursor 3AB. J. Biol. Chem. **269:**27015–27020.
40. **Murphy, J. F., R. E. Rhoads, A. G. Hunt, and J. G. Shaw.** 1990. The VPg of tobacco etch virus RNA is the 49 kDa proteinase or the N-terminal 24 kDa part of the proteinase. Virology **178:**285–288.
41. **Pata, J. D., S. C. Schultz, and K. Kirkegaard.** 1995. Functional oligomerization of poliovirus RNA-dependent RNA polymerase. RNA **1:**466–477.
42. **Paul, A. V., X. Cao, K. S. Harris, J. Lama, and E. Wimmer.** 1994. Studies with poliovirus polymerase $3D^{pol}$: stimulation of poly(U) synthesis in vitro by purified poliovirus protein 3AB. J. Biol. Chem. **269:**29173–29181.
43. **Raikhel, N. V.** 1992. Nuclear targeting in plants. Plant Physiol. **100:**1627–1632.
44. **Restrepo, M. A., D. D. Freed, and J. C. Carrington.** 1990. Nuclear transport of plant potyviral proteins. Plant Cell **2:**987–998.
45. **Restrepo-Hartwig, M. A., and J. C. Carrington.** 1992. Regulation of nuclear transport of a plant potyvirus protein by autoproteolysis. J. Virol. **66:**5662–5666.
46. **Restrepo-Hartwig, M. A., and J. C. Carrington.** 1994. The tobacco etch potyvirus 6-kilodalton protein is membrane-associated and involved in viral replication. J. Virol. **68:**2388–2397.
47. **Riechmann, J. L., S. Laín, and J. A. García.** 1992. Highlights and prospects of potyvirus molecular biology. J. Gen. Virol. **73:**1–16.
48. **Roberts, B.** 1989. Nuclear location signal-mediated protein transport. Biochim. Biophys. Acta **1008:**263–280.
49. **Schaad, M. C., R. Haldeman-Cahill, S. Cronin, and J. C. Carrington.** 1996. Analysis of the VPg-proteinase (NIa) encoded by tobacco etch potyvirus: effects of mutations on subcellular transport, proteolytic processing, and genome amplification. J. Virol. **70:**7039–7048.
50. **Shahabuddin, M., J. G. Shaw, and R. E. Rhoads.** 1988. Mapping of the tobacco vein mottling virus VPg cistron. Virology **163:**635–637.
51. **Slade, D. E., R. E. Johnston, and W. G. Dougherty.** 1989. Generation and characterization of monoclonal antibodies reactive with the 49-kDa proteinase of tobacco etch virus. Virology **173:**499–508.
52. **Toyoda, H., C.-F. Yang, N. Takeda, A. Nomoto, and E. Wimmer.** 1987. Analysis of RNA synthesis of type 1 poliovirus by using an in vitro molecular genetic approach. J. Virol. **61:**2816–2822.
53. **Wimmer, E., C. U. Hellen, and X. Cao.** 1993. Genetics of poliovirus. Annu. Rev. Genet. **27:**353–436.
54. **Xiang, W., A. Cuconati, A. V. Paul, X. Cao, and E. Wimmer.** 1995. Molecular dissection of the multifunctional poliovirus RNA-binding protein 3AB. RNA **1:**892–904.
55. **Xiang, W., K. S. Harris, L. Alexander, and E. Wimmer.** 1995. Interaction between the 5′-terminal cloverleaf and $3AB/3CD^{pro}$ of poliovirus is essential for RNA replication. J. Virol. **69:**3658–3667.